Atten Percept Psychophys (2015) 77:1170–1188
DOI 10.3758/s13414-015-0832-6

Different developmental trajectories across feature types support a dynamic field model of visual working memory development

Vanessa R. Simmering · Hilary E. Miller · Kevin Bohache

Published online: 4 March 2015

Abstract Research on visual working memory has focused on characterizing the nature of capacity limits as "slots" or "resources" based almost exclusively on adults' performance with little consideration for developmental change. Here we argue that understanding how visual working memory develops can shed new light onto the nature of representations. We present an alternative model, the Dynamic Field Theory (DFT), which can capture effects that have been previously attributed either to "slot" or "resource" explanations. The DFT includes a specific developmental mechanism to account for improvements in both resolution and capacity of visual working memory throughout childhood. Here we show how development in the DFT can account for different capacity estimates across feature types (i.e., color and shape). The current paper tests this account by comparing children's (3, 5, and 7 years of age) performance across different feature types. Results showed that capacity for colors increased faster over development than capacity for shapes. A second experiment confirmed this difference across feature types within subjects, but also showed that the difference can be attenuated by testing memory for less familiar colors. Model simulations demonstrate how developmental changes in connectivity within the model—purportedly arising through experience—can capture differences across feature types.

Keywords Visual working memory · Capacity · Neural network model · Development · Change detection

Significance: Two studies with children suggest that slots and resource models are under-specified to account for developmental increases in capacity and differences in memory across feature types. Our results indicate higher capacity for colors than shapes emerging over development. Slot models have not addressed differences across feature types, but the characterization of discrete, high-resolution representations suggests no differences. Although resource accounts can explain variation in capacity across feature types, they include no mechanism by which this difference would emerge developmentally. Simulations of an alternative model, the dynamic field theory, demonstrate the utility of process-based models in understanding visual working memory development.

V. R. Simmering (✉) · H. E. Miller
Department of Psychology and Waisman Center, University of Wisconsin-Madison, Madison, WI, USA
e-mail: simmering@wisc.edu

V. R. Simmering
McPherson Eye Research Institute, University of Wisconsin-Madison, Madison, WI, USA

K. Bohache
Department of Psychology, University of Iowa, Iowa City, IA, USA

A well-known characteristic of visual working memory (VWM) is its limited capacity (estimated to be three to five simple objects; Cowan, 2001), but the nature of this limitation has been a source of considerable debate. The focus of this debate has been on whether slot-like, fixed-resolution representations (e.g., Zhang & Luck, 2008), or the allocation of a limited resource pool with decreasing resolution per item as the number of items increases (e.g., Bays & Husain, 2008), provides a more complete account of performance in laboratory tasks. Although dozens of studies have been published and some empirical support has been found for each approach, as well as for some hybrid approaches (e.g., Alvarez & Cavanagh, 2004; Xu & Chun, 2006) , the debate has not yet been resolved.

In this paper, we argue that an important dimension in this debate that has been largely ignored is the nature of developmental change. Specifically, we propose that understanding how capacity increases over development will shed light onto the nature of the underlying VWM representations. Empirical studies have demonstrated improvements in working memory with age, but few theories have proposed specific mechanisms that underlie developmental increases in capacity (see

Simmering & Perone, 2013, for review). The source of developmental changes in VWM has important implications not only for understanding how VWM functions in adults, but also for potential insight into atypical populations who show deficits in VWM (e.g., with schizophrenia and attention-deficit/hyperactivity disorder (Karatekin & Asarnow, 1998), or following preterm birth (Luciana, Lindeke, Georgieff, Mills, & Nelson, 1999)). Furthermore, studies on working memory training suggest that earlier interventions may be more beneficial (Wass, Scerif, & Johnson, 2012), but that we need a better understanding of how working memory functions and develops to create effective interventions (e.g., Shipstead, Hicks, & Engle, 2012).

In the sections that follow, we first review how VWM develops and the theories that have been put forth to explain both capacity and development. Next, we present the Dynamic Field Theory (DFT) as an alternative model to the dominant slots and resources perspectives (Johnson & Simmering, in press; Johnson, Simmering, & Buss, 2014). The DFT incorporates a specific developmental mechanism that can account for developmental improvements in both capacity (Perone, Simmering, & Spencer, 2011; Simmering, 2008, 2015) and resolution (Simmering & Patterson, 2012) of color memory. Here we test this model further by considering how memory differs across feature types and potential sources of these differences.

Development of VWM

The primary task used to assess capacity in children is the change detection task (e.g., Cowan et al., 2005; Riggs, McTaggart, Simpson, & Freeman, 2006; Riggs, Simpson, & Potts, 2011; Simmering, 2012). In this task, a small number of simple items are shown briefly (e.g., 500 ms–2 s) in a memory array, followed by a short delay (e.g., 1 s). Then, a test array is presented in which either all of the items match the memory array or one item has changed; children are instructed to respond *same* or *different* accordingly. Capacity is estimated from children's responses across trial types (e.g., with the formula proposed by Pashler, 1988; or modified by Cowan, 2001). Together these studies have demonstrated a gradual increase in VWM capacity between 3 and 12 years of age.

Most studies employing the change detection task with children have either implicitly or explicitly endorsed a slot-like explanation for capacity, with results indicating an increase in the number of slots over development (e.g., Cowan, Morey, Chen, Gilchrist, & Saults, 2008). According to "slots" explanations of VWM capacity, most errors in performance arise when an item is not stored in memory because the number of items to be remembered exceeds the number of available memory slots. As a potential neural instantiation of slots, Raffone and Wolters (2001; see also Vogel, Woodman, & Luck, 2001) proposed that objects are represented through simultaneous firing of neurons in "cell assemblies" that correspond to the various features (e.g., color, orientation, location) of a given object. To represent multiple objects, cells must fire in synchrony with other cells representing the same object, but not with cells representing other objects. Thus, as the number of objects increases, the temporal segregation of the assemblies associated with each object becomes more difficult, resulting in mis-synchronizations and errors.

What remains unclear within a slots view, however, is what causes a new slot to develop. Riggs et al. (2011) suggested changes in neural synchrony as a possible source of developmental increases in capacity. They described two possible ways that accidental mis-synchronization could decrease over development: (1) the neural assemblies coding for each object may become better synchronized, thus increasing the differentiation between items; or (2) connections between cell assemblies may be selectively reduced, thereby decreasing the potential for mis-synchronization across objects. By this account, capacity should be the same across objects with different feature types. Studies with children have almost exclusively tested memory for colored squares (e.g., Cowan et al., 2005; Riggs et al., 2006; Simmering, 2012), although one study used white shapes (Simmering, 2015, see also 2008) and another compared performance on orientation versus both orientation and color when presenting colored oriented bars (Riggs et al., 2011). These studies did not include statistical comparison between color and shape or orientation, so it is unknown whether capacity is comparable across feature types during childhood.

Another type of paradigm has been used to assess the resolution or precision of VWM over development. Burnett Heyes and colleagues tested 7- to 13-year-olds boys' memory for oriented bars (Burnett Heyes, Zokaei, van der Staaij, Bays, & Husain, 2012). In this task, children were shown one or three oriented bars on each trial, and were asked to reproduce the orientation of one bar after a short delay. Results showed that precision was higher when remembering one versus three bars, and precision improved over development, with more improvement on three-bar trials. Using a resource-based explanation, the authors argued that VWM is not limited in capacity, but rather impairments in performance arise through limitations in resolution. From this perspective, VWM is a continuous resource that can be flexibly allocated across different numbers of items held in memory. As the number of items increases, the resolution of each item decreases, which explains the increase in errors as set size increases. Burnett Heyes et al. suggested that the resolution of memory resources improves over development, and that such an increase in resolution might result from "sharpening" of representations within neural populations that sub-serve VWM tasks. However, the manner in which changes in

neural populations would result in resolution changes is not specified.

Simmering and Patterson (2012) developed a color discrimination task, similar to a single-item change detection task, that tested children's ability to detect very small changes in color after a short memory delay. Their results demonstrated that discrimination thresholds (i.e., the difference in color necessary to reliably elicit "different" judgments) decreased between 4 and 6 years and again to adulthood, indicating a developmental increase in the resolution of memory for a single color. Rather than subscribing to a resource-based explanation, however, they proposed that the change in resolution arises through the same mechanism that can account for increases in capacity. Their account of VWM capacity and development, the Dynamic Field Theory (DFT; Johnson & Simmering, in press; see Johnson et al., 2014, for specific contrasts with slot and resource perspectives), is a process-based neural network model in which visual information (i.e., color) is represented within continuous dynamic neural fields (see Edin et al., 2009; Wei, Wang, & Wang, 2012, for similar types of representations).

In the DFT, combining two excitatory neural fields with a shared inhibitory neural field produces a three-layer architecture in which an excitatory contrast field processes visual information in the scene and an excitatory working memory field maintains visual information in the absence of input. These representations are realized as localized "peaks" of activation within the excitatory fields; peaks are maintained through local excitatory connections that keep activation above threshold (zero) and lateral inhibitory projections that prevent activation from spreading throughout the field. Neural interactions between the contrast and inhibitory fields are tuned such that peaks in the contrast field are input-driven, that is, when input is removed, activation relaxes back to its resting level. In the working memory field, by contrast, excitatory and inhibitory interactions are much stronger, allowing for self-sustaining peaks that are maintained robustly after input is removed.

Figure 1 shows how the DFT performs the change detection task with parameters tuned to capture adults' performance (see Table 1 for parameters and Appendix for model equations). When three items are presented to the model, they form self-sustaining peaks in the working memory field (Fig. 1A). The shared inhibitory layer projects to the corresponding color values in the contrast field, which produces inhibitory troughs at these locations when input is removed (i.e., during the delay; Fig. 1B). When the test array is presented, if no items have changed, the familiar colors project into these inhibited regions of the contrast field (see Fig. 1C). This serves as the comparison process in the DFT—if a new color is presented, this input projects into un-inhibited regions of the contrast field to build input-driven peaks (see circle in Fig. 1D). To generate the *same/different* response required in change detection, a simple decision system is linked to the three-layer network such that activation in the contrast field drives a *different* response and activation in the working memory field drives a *same* response. The decision nodes compete in a winner-take-all fashion to generate a discrete response—when activation of one node surpasses zero—on each trial. In the sample simulations in Fig. 1, the three familiar items produce a correct *same* response (see dotted line in Fig. 1E), whereas the new item produces a correct *different* response (see solid line in Fig. 1F).

Johnson, Simmering, and Buss (2014) conducted quantitative simulations demonstrating how this model can capture adults' performance in the change detection task, and contrasted the model with slots and resource perspectives. The DFT aligns with some characteristics of slots (i.e., discrete, all-or-none encoding of items) and resources (i.e., variable resolution of items in memory across set sizes), but moves beyond these theories in accounting for the processes of comparison and decision generation necessary to perform the change detection task. Capacity in the DFT is limited by the balance between excitation and inhibition in the working memory field: as more items are added, the excitation from the peaks in the working memory field projects to the shared inhibitory layer, which then projects back into the working memory field. At some point, no additional peaks can be sustained within the working memory field due to the strength of inhibition.

Simmering (2008) showed how the model could account for developmental increases in VWM capacity through a strengthening of interactions both within and between the layers of the model and the decision nodes (see Simmering & Schutte, in press, for further discussion). Figure 2 shows sample simulations with parameters tuned to capture 5-year-olds' performance (i.e., behavioral data from Simmering, 2012; see also Simmering, 2015). Compared to Fig. 1, it is apparent that both excitation and inhibition are weaker in the "child" model than in the "adult" model. The model's performance is still correct the majority of the time, but the likelihood of errors is higher, capturing children's more error-prone performance. Simmering (2008, 2015) found that errors in the child model arose through multiple sources: failure to encode all of the items (especially at higher set sizes), loss of an item during the delay, a weak signal to the decision nodes, and/or noisy competition in the decision system. The simulation in Fig. 2D illustrates how the signal to the decision nodes is weaker; although the model produced a correct "different" response on this trial, the input-driven peak in the contrast field was quite weak. Across many trials, this low level of activation (relative to the adult parameters; cf. Fig. 1D) leads to more errors.

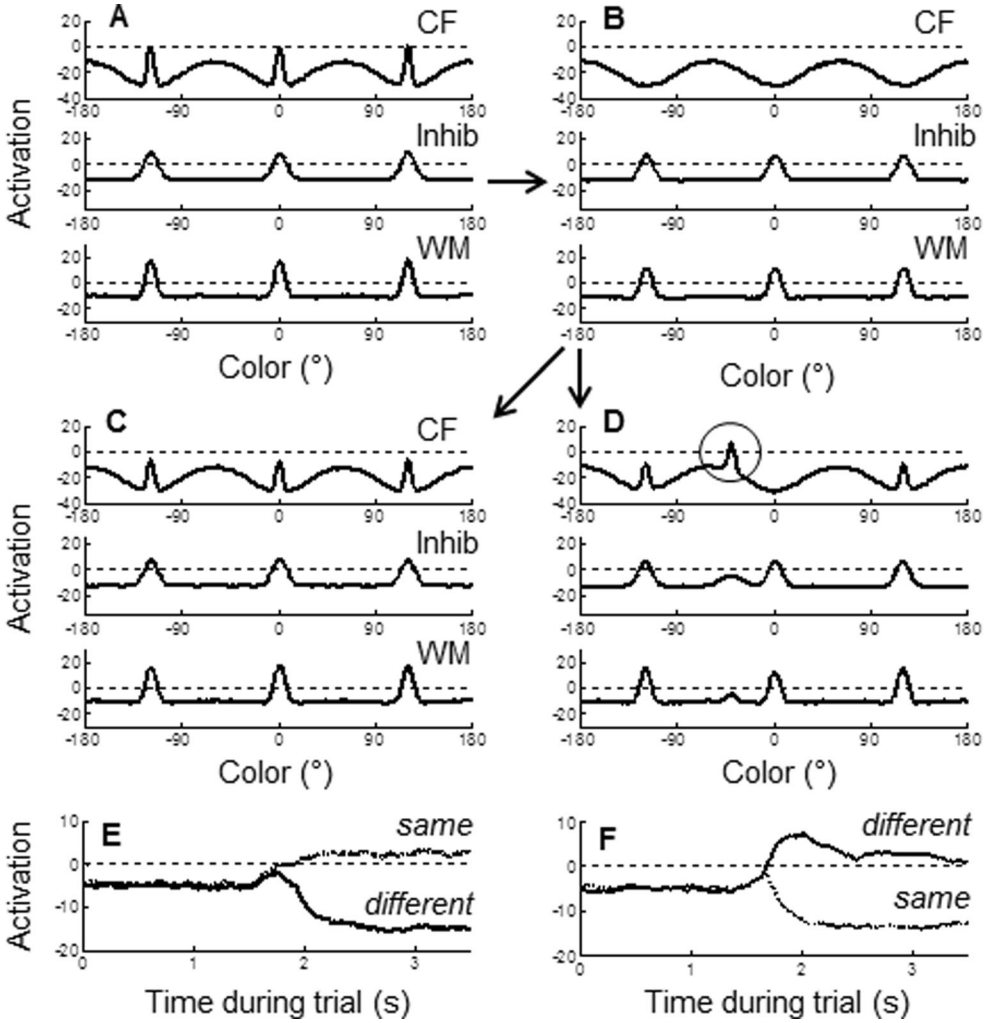

Fig. 1 Time slices through the three layers of the model, run with "adult" parameters, at critical points in two trials: (**A**) encoding, at the end of memory array presentation; (**B**) maintenance, at the end of delay; comparison at the time just before a response is generated during presentation of the test array on (**C**) no-change and (**D**) change trials; and activation of the decision nodes (dotted = *same*, solid = *different*) on the (**E**) no-change and (**F**) change trials. Arrows indicate progression through the trials. Dashed black lines in each panel indicated the activation threshold (i.e., 0). CF = contrast field, WM = working memory field

Simmering (2015) simulated 3-, 4-, and 5-year-olds' and adults' performance by changing 18 parameters (out of 51 total parameters; cf. Tables 1 and 2) to be weaker earlier in development. These simulations provided the first mechanistic explanation for capacity increases during early childhood, showing how these changes in connectivity led to not only increases in the number of items (peaks) that could be held in working memory, but also better accuracy in the comparison and decision processes (see Simmering & Schutte, in press, for further discussion). This account also led to the predictions tested by Simmering and Patterson (2012), that the precision of memory should improve in parallel to increases in capacity due to the same underlying developmental mechanism. Thus, the DFT accounts for improvements in both resolution and capacity through the same developmental mechanism: strengthening connectivity.

One question raised by the developmental change implemented in the DFT is what drives changes in the strength of connections in the model. Perone and Spencer (2013a) showed that a Hebbian learning mechanism in the DFT could produce the types of changes previously implemented "by hand" (i.e., by the modeler specifying parameter values separately for different age groups; see Simmering & Schutte, in press, for further discussion). In particular, they demonstrated that simulating extended experience with a variety of stimuli led to a distribution of learning that supported later visual processing of similar stimuli. These simulations suggest that differential experience should lead to differential rates of development.

Here we extend these findings from distributed experience along a single dimension (i.e., color) to

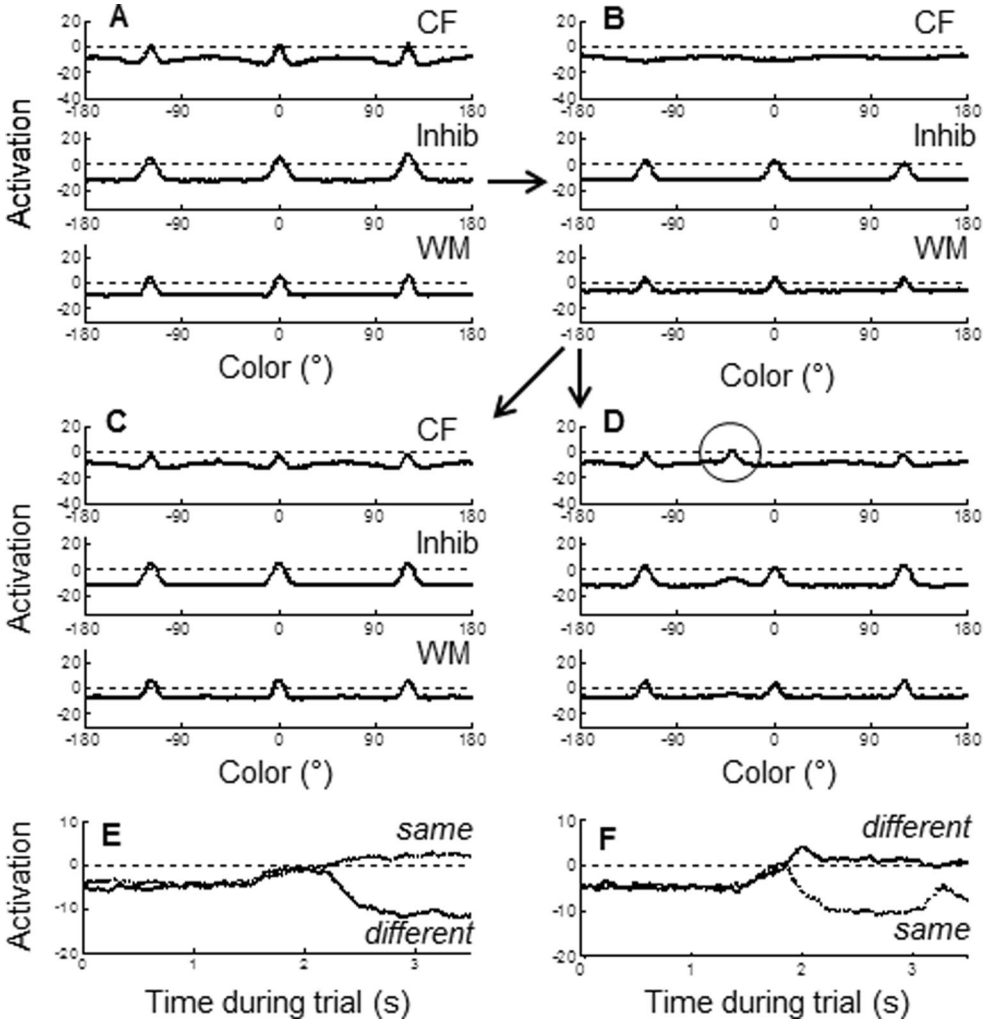

Fig. 2 Time slices through the three layers of the model, run with "child" (5-year-old) parameters, at critical points in two trials; panels and axes are as in Fig. 1

comparisons across different dimensions (e.g., shape and color). Such differential development could explain an effect that has been previously demonstrated but not yet explained: adults show VWM capacity differences depending on feature types (e.g., higher for colors than shapes; Wheeler & Treisman, 2002, Experiment 4). We hypothesize that more common features are processed (perceived and remembered) more frequently than less common features, leading to slightly accelerated development and therefore higher capacity. This explanation is similar to knowledge accounts in verbal working memory research in which children's experience with words allows them to remember more (see Miller, 2013, for review). Studies of VWM development have not explicitly addressed whether and how performance differs across single feature types. However, Simmering (2008, see also 2015) tested separate groups of participants in change detection tasks using colored squares or white shapes across experiments. Although these experiments were not compared statistically, reported means suggested slightly higher capacity for colors than for shapes in both children (3- 4-, and 5-year-olds) and adults.

Testing the DFT account of development across features

To test whether the model can quantitatively capture performance across feature types through more or less developed memory, we began with parameters tuned to capture 5-year-olds' performance on colors (Simmering, 2015; see Table 2). Next, we adjusted a small number of parameters (three out of seven strength parameters that varied over development; see *General discussion* for details on the choice of parameters to modify) to be weaker in the fields to represent shape relative to

color[1]; the parameters for the formation of long-term memory and the decision system were held constant across feature types (see Appendix for full details). We tuned these three parameters to fit 5-year-olds' performance on shapes (Simmering, 2008, 2015). Behavioral estimates of capacity were 2.87 for color and 2.28 for shape; model simulations produced estimates of 2.88 for color and 2.67 for shapes (see Table 3 for correct rejection and hit rates across set sizes, along with mean absolute error to evaluate the overall fit). As this comparison shows, we fit 5-year-olds' performance across feature types by modifying the parameters to be less developed for shape than color. Thus, the DFT can account for differences in performance across feature types through developmental differences in memory for the features.

We then tested an extension of this finding by taking the parameters tuned to 3- and 7-year-olds' performance on colors (i.e., behavioral data from Simmering, 2012; see Table 2 for parameter values and Table 4 for evaluation of fits) and modified them proportionally to the 5-year-old parameters. Specifically, the three parameters we modified to fit shape performance were the strength of input, the strength of self-excitation in working memory, and the strength of inhibition projected to working memory; the values for the shape parameters were approximately 97 % the strength of the corresponding color parameters, respectively. To predict 3- and 7-year-olds' performance on shapes, then, we scaled these three parameters to be 0.97 for each "age" to simulate memory for shapes. Using the scaled 3-year-olds parameters, we found capacity estimates of 1.84 for color and 1.72 for shape; with the 7-year-old scaled parameters, estimates were 3.95 and 3.30, respectively. As these simulations show, the model produced an advantage of color over shape for each age group (differences of 0.12 for 3-year-olds, 0.21 for 5-year-olds, and 0.65 for 7-year-olds) with the difference between features increasing with age.

How does this account compare to other theories of VWM capacity and development? This is a difficult question to answer with certainty because few papers have addressed whether and why performance differs by feature type. We found no developmental papers that compared capacity across single feature types; rather, a few papers have addressed a related debate, focusing on why adults' capacity appears lower for complex objects (e.g., Chinese characters, irregular polygons) than for simple objects (e.g., colored squares, letters). These results have been interpreted as evidence that VWM is limited by information load, specifically, that more complex items require more information to be encoded (Alvarez & Cavanagh, 2004). However, complexity was confounded with inter-item similarity in these studies, and the differences in performance can be eliminated when changes are sufficiently large, suggesting that capacity did truly not differ between object types (Awh, Barton, & Vogel, 2007). Wheeler and Treisman (2002) argued for parallel memory stores for color versus shape, each with its own limited (slot-like) capacity, but did not specify what led to greater capacity for one feature over the other. Bays, Wu, and Husain (2011) presented evidence for independence between memory for the color versus orientation of stimuli, leading them to conclude that each feature was represented by a separate pool of resources. Whether there should be differences in resolution of items along these dimensions, however, was not specified. As such, explanations within the literature have accommodated for possible differences across feature types without explicitly hypothesizing the source of such differences.

In the DFT, the specific account of developmental increases in capacity can be extended to the prediction that differences across feature types could arise through experience over development. By contrast, slot and resource accounts provide no specific hypotheses to account for why performance would differ across feature types and how this difference could emerge over development. We tested the DFT account with two experiments. In Experiment 1 we tested multiple age groups in a change detection task with shapes as stimuli. We compared capacity for shapes to color capacity (from Simmering, 2012) to test for the developmental emergence of a difference across features. As predicted, we found that capacity was higher for colors than shapes, especially in older children. As a further test of developmental emergence, we designed Experiment 2a to compare feature types within participants, replicating greater capacity for colors than shapes. In Experiment 2b, we modified the color stimuli to be less familiar; consistent with the experience account of feature differences, this showed lower capacity than canonical colors.

Experiment 1

For our first experiment, we used a change detection task to test memory for white shapes in 3-, 5-, and 7-year-old children. Previous results using these age groups showed increases in capacity for color between 3 and 5 and between 5 and 7 years (Simmering, 2012), suggesting that these age groups should provide a good range of comparison.

[1] Although Perone and Spencer (2013a) used autonomous developmental change to show the effect of experience on visual processing, it would be impractical to generate fits in such a way for the current studies. Perone and Spencer were simulating infants' experience on the order of months, whereas we would be simulating experience over multiple years. Our primary simulation computer took approximately 1.5 hours to simulate 20 "participants" in the change detection task; simulating the amount of experience accumulated over many years is unattainable with our current computational power.

Furthermore, by testing the same age groups as Simmering (2012), we can compare results across studies for differences between feature types.

Method

Participants Forty-nine children participated in this experiment: 15 were 3-year-olds (M age =3.70 years, SD = 2.72 months, eight girls and seven boys), 18 were 5-year-olds (M age = 5.25 years, SD = 3.99 months, nine girls and nine boys), and 16 were 7-year-olds (M age = 7.50 years, SD = 2.96 months, eight girls and eight boys). An additional 13 children participated but were excluded for the following reasons: six did not follow task instructions (three 3-year-olds, three 7-year-olds) and seven had insufficient data due to ending their participation early (four 3-year-olds, one 5-year-old) or equipment failure (two 7-year-olds). Parents of all participants reported normal or corrected-to-normal visual acuity and no family history of colorblindness. Participants were recruited through a database of families interested in research participation compiled by a university affiliated research center and received a small gift following participation.

Apparatus Stimuli were modeled after the eight white shapes from Wheeler and Treisman (2002), and are shown in Fig. 3A. Items were selected randomly without replacement for the memory and for the new item needed for the test array on change trials.

The task was explained to children as a card-matching game using flashcards (3 in × 3 in. that showed set sizes one, two, and three (see Simmering, 2012, for details of development of the "card" version of the task for young children). For most participants (n = 32), the computerized trials were completed on a 15.4-in widescreen Dell Latitude E6500 laptop computer, with stimulus presentation controlled by Matlab 10.2 using the Psychophysics Toolbox extension (version 3; Kleiner, Brainard, & Pelli, 2007). For the remaining participants (n = 14), these trials were completed on an 18-in CRT display connected to a Macintosh G4 computer, with stimulus presentation controlled by Matlab 5.2 (Mathworks, Inc., http://www.mathworks.com) using the Psychophysics Toolbox extensions (version 2; Brainard, 1997; Pelli, 1997). In both cases, lighting in the room was dimmed to aid viewing of the screen, and stimulus presentation was adjusted to appear approximately the same size on both screens.

Children were seated in a child-sized desk chair, at a viewing distance of approximately 2 f. from the computer screen.[2] The background on the computer monitor was black, and the stimuli were enclosed within gray rectangular "card" frames (5.75 in tall × 4.75 in wide; approximately 13.5° × 11.2° visual angle). The gray frame was centered vertically on the screen on every trial; each block began with the frame centered horizontally on the left half of the screen, and alternating sides over trials, as shown in Fig. 4. Within the frame, stimuli (1 in or ~2.4° square bitmaps) could appear at any of five equally-spaced positions in a circle (3 in or ~7° diameter) around the center of the frame. For set sizes two, three, and four, the stimuli appeared in neighboring positions; all five positions were filled for set size five. For each set size, the positions were chosen randomly for the first trial, but remained constant across the trials within that set size (note that trials were blocked by set size, as described below).

Procedure An experimenter described the task to children as a matching game in which the child needed to look for cards that match. For training, the experimenter demonstrated the task using flashcards showing one, two, or three items. The first card in each set was shown for approximately 2 s, and the child was instructed to "Look at the picture and remember what it shows"; the terminology "picture" was used to build on children's experience playing commercially available picture-matching card games, and to emphasize the need to compare arrays separated in time, rather than comparing multiple objects within a single array. The first card was then removed and, after a brief delay, the second card for the trial was shown in the same location. The experimenter then asked the child if the two cards matched. After the child responded, the experimenter placed both cards side-by-side and praised or corrected the child as needed, explicitly pointing out the changed item to ensure the child understood the proper comparison. The flashcard trials were presented in ascending order of set sizes one, two, and three, with the order of change and no-change trials counter-balanced across set sizes. During training, the experimenter emphasized that all items in the display must match to be considered *same*. Most 3-year-olds did not complete set sizes greater than three (cf. Simmering, 2012), so higher set sizes were not presented on the flashcards. For 5- and 7-year-olds, flashcards for set sizes four and five were presented immediately before the test block, rather than during training, for these set sizes.

Once the child understood the task, the experimenter began the computerized version. Note that many studies using the change detection task with adults include articulatory suppression (e.g., repeating a three-digit number) to prevent verbal recoding of the stimuli (e.g., Vogel et al., 2001). Developmental studies of visuospatial working memory have shown that children do not typically recode visual information verbally (see Pickering, 2001, for review); furthermore, studies that have included articulatory suppression with children have shown no effects for the age groups used here (e.g., Hitch, Woodin, & Baker, 1989; Miles, Morgan, Milne, & Morris, 1996). As such, we chose not to require articulatory

[2] Children typically move their heads and bodies much more than adults while participating in the task, which precludes the calculation of precise visual angels for the stimulus presentations. We have provided approximate calculations, but these may have varied across child participants depending on movement.

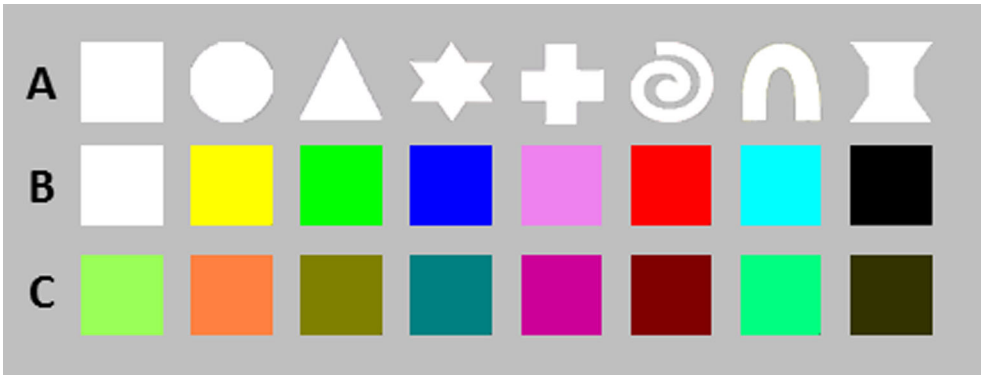

Fig. 3 Stimuli used in the current paper: (**A**) white shapes were used for Experiment 1 and the shape conditions of Experiments 2a and 2b; (**B**) colored squares for Experiment 2a (also in Simmering, 2012); (**C**) unfamiliar colors for Experiment 2b. Note that the differences between colors may appear smaller in print versions than on the computer screen used in the task

suppression in our task. The first block consisted of practice trials, with the memory array presented for 2 s, a delay of 900 ms, and the test array presented until a response was entered. Children verbally responded "same"/"different," "yes"/"no," or "match"/"no match" (terms that are more intuitive for 3-year-olds), and the experimenter entered the response on a keyboard. When the response was entered, a chime played if it was correct, to help children stay motivated. Each trial was initiated with a key press by the experimenter when the child appeared ready, to allow for the participants to control the pacing of the task as needed. If children seemed fatigued, they were offered a break between set size blocks; 3-year-olds were also offered small prizes (e.g., bubbles, stickers, Play-Doh) between trial blocks to maintain their motivation.

The practice block included eight trials in random order: four trials in set size one and four trials in set size two; for all blocks, the computer program randomly chose whether each trial was change or no-change, which resulted in roughly equal but slightly different numbers of each trial type across blocks and participants. Following the practice block, children began the test trials, which differed from the practice trials in that a shorter presentation time (500 ms) was used for the memory array for 5- and 7-year-olds; the longer memory array (2 s) was used for younger children to ensure they had time to orient and attend to the display, as younger children tend to spend more time off task between trials (Simmering, 2012).[3] The test blocks each included 12 trials at a single set size, and were ordered the same for all children: set size two, one, three, four, five. Simmering (2008) found that this order maximized young children's attention to all of the items in the higher set sizes as well as their likelihood to complete test blocks at least up to set size three. Whenever possible, we included children's data from completed trial blocks if the child chose to end early (see Results section for details). The total duration of the task was approximately 20–30 min.

[3] Due to experimenter errors, the wrong stimulus presentation duration was used for one 3-year-old and 14 of the 5-year-olds; previous studies have suggested that stimulus duration does not significantly influence capacity (Cowan, AuBuchon, Gilchrist, Ricker, & Saults, 2011; Vogel, Woodman, & Luck, 2001), so we do not expect this to affect our results.

Results and discussion

Participants' responses were classified as correct rejections (correct no-change trials), hits (correct change trials), misses (incorrect change trials), and false alarms (incorrect no-change trials). Figure 5 shows the distribution of these response types separately for each age group, with response distributions from Simmering (2012) for comparison. Note that correct rejections and false alarms sum to 1.0 (no-change trials) and hits and misses sum to 1.0 (change trials). As this figure shows, correct rejection and hits (i.e., correct responses) were most common, especially at low set sizes; as set size increased, errors increased, especially misses. Across age groups, this decline in performance occurred at smaller set sizes for younger children, and higher set sizes for older children. Note that all age groups showed more of a decrease in hits than correct rejections, similar to adults' pattern of performance (cf. Vogel et al., 2001); this suggests that children are approaching the task as adults do, not responding randomly, despite their overall worse performance (Simmering, 2012). Comparing feature types, performance appears superior for colors versus shapes.

One significant challenge in comparing performance across this range of development is that younger children were typically unable to complete blocks at set sizes higher than three; thus, comparing performance across set sizes and age groups is truncated to only low set sizes, where performance is near ceiling for older age groups. Although this type of comparison does reveal some differences across age groups, it does not encompass the full pattern of performance for older children. One solution to this problem is to compute a measure that is based on

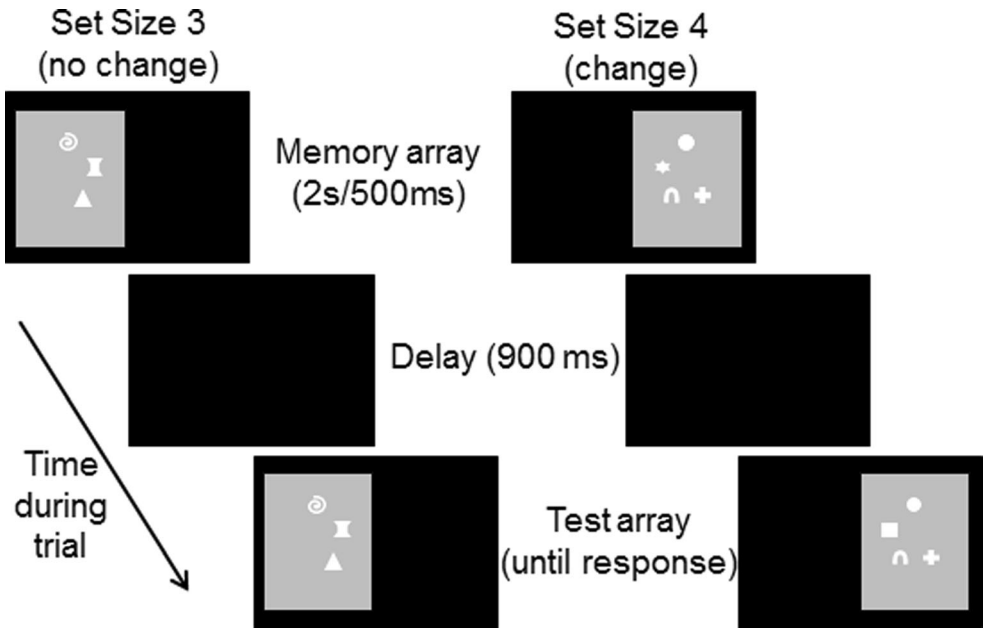

Fig. 4 Examples of stimulus presentation in a no-change trial (**left**) and a change trial (**right**) from Experiment 1. Note that stimuli are not drawn precisely to scale

performance across set sizes but yields a single value for each participant. This can be achieved by computing a capacity estimate K for all completed set sizes, then selecting each participant's maximum K across set sizes (K_{max}) as an index of their capacity (described further below). Simmering (2012) showed that the K_{max} estimate for each participant does not necessarily come from the highest set size that participant completed. Furthermore, when analyzing performance across set sizes for each age group separately, Simmering demonstrated that significant decreases in percentage correct corresponded roughly to mean K_{max} estimates for that age group (i.e., both 3- and 5-year-olds' performance declined significantly between set sizes two and three, and their mean K_{max} estimates were 1.90 and 2.90 items, respectively; 7-year-olds' performance declined significantly between set sizes three and four, with a K_{max} estimate of 3.91 items). Thus, comparing the mean K_{max} estimates across age groups can avoid limitations arising from young children's completion of fewer set sizes than older children.

We computed capacity (K) for each participant using Pashler's (1988) formula, $K = SS * (H - FA) / (1 - FA)$, based on the hit ($H$) and false alarm ($FA$) rates for each set size (SS). Because K can equal, at most, the set size for each block, we then selected each participant's maximum estimate across set sizes (cf. Olsson & Poom, 2005; Simmering, 2012), to derive K_{max} for each participant. Mean K_{max} estimates for each age group and condition are shown in Fig. 6A. As this figure shows, K_{max} was lower for the current experiment using shapes compared to the color condition from Simmering (2012) for older children. We analyzed these data for comparison with Simmering's (2012) color results in a two way ANOVA with Feature (shape, color) and Age Group (3 years, 5 years, 7 years) as between-participants factors. This analysis revealed a significant main effect of Age Group, $F_{2, 85} = 41.75$, $p < .001$, $\eta_p^2 = .44$. Tukey follow-up HSD tests ($p < .05$) showed that K_{max} differed significantly between all three age groups.[4] This analysis also revealed a significant main effect of Feature, $F_{1, 85} = 17.58$, $p < .001$, $\eta_p^2 = .09$, with overall higher capacity for colors ($M = 2.91$) than shapes ($M = 2.31$). The interaction showed a trend toward significance, $F_{2, 85} = 1.81$, $p = .170$, with the gap between feature types increasing over development. Planned comparisons (two-tailed independent samples t-tests) across feature types within each age group showed no difference for the 3-year-olds ($t_{27} = 1.47$, $p = .153$), but significantly higher capacity for colors than shapes for both 5-year-olds ($t_{30} = 2.12$, $p = .042$, $d = .76$) and 7-year-olds ($t_{28} = 3.46$, $p = .002$, $d = 1.25$).

Figure 6B shows the capacity estimates resulting from the DFT simulations described above. As this figure shows, the pattern from the model was similar to the pattern obtained in with the behavioral data (recall that the shape performance for 3- and 7-year-olds was a prediction generated from scaled parameters, not fit to behavioral data). Our findings of higher capacity for colors than shapes in older children is consistent with the models performance and similar to adults' performance

[4] To ensure that this effect wasn't driven solely by Simmering's (2012) similar finding across age groups, we also tested for an effect of age group in the shape condition alone; this analysis revealed the same pattern, $F_{2, 46} = 17.27$, $p < .001$, $\eta_p^2 = .43$, with all age groups differing significantly from each other (Tukey HSD $p < .05$).

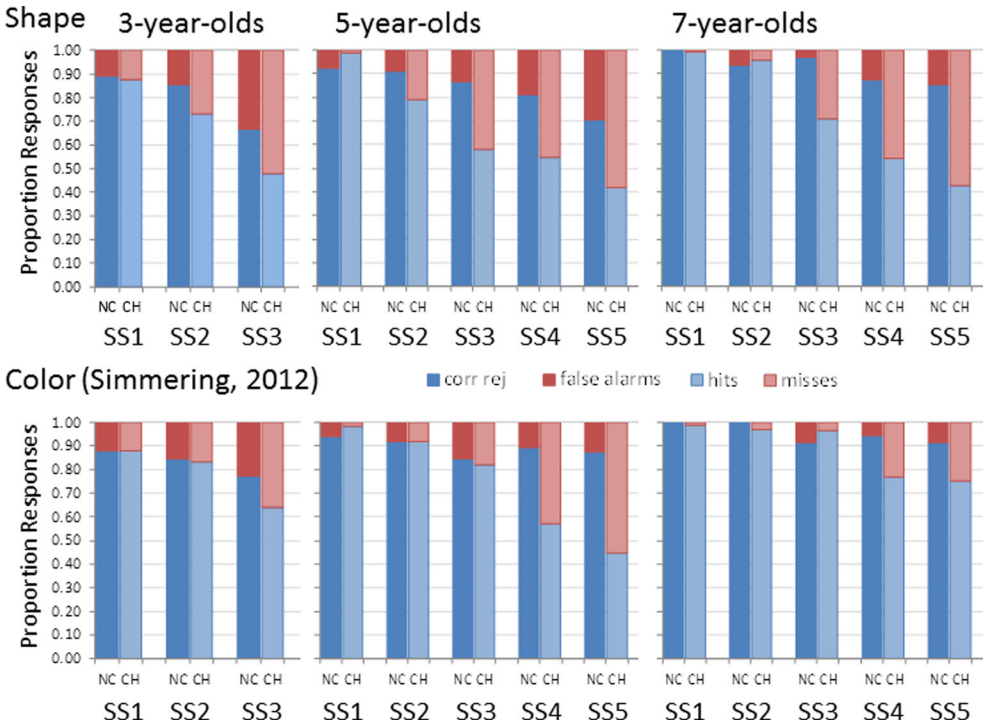

Fig. 5 Proportions of response types across set sizes, separated by age groups (columns) and experiments (rows) for Experiment 1, with Simmering (2012) for comparison. Corr rej = correct rejections; SS = set size; NC = no-change trials; CH = change trials

in the change detection task (e.g., Wheeler & Treisman, 2002). These results provide initial support for our hypothesis that the difference in performance across feature types arises through experience over development. One limitation of the current study, however, is that we compared feature types across different groups of children; Wheeler and Treisman, by contrast, compared feature types within participants. Our next experiment was designed to test whether this difference across features would replicate within a single group of participants (2a), and whether the specific values along a feature dimension matter (2b).

Experiment 2

To test whether the difference in capacity estimates for colors versus shapes in Experiment 1 was robust, we conducted a within-participant comparison of these features in Experiment 2a. The fact that children are only able to complete a relatively small number of trials within a testing session introduced some practical challenges to collecting data. Because 7-year-olds were the only age group to reliably complete all five set sizes tested in Experiment 1, we chose to test only this age group in the current experiment. Then, for Experiment 2b, we tested the DFT account of development arising through experience by using less-familiar colors on the color trials. If the superior performance on color versus shape is driven by relatively more developed feature representation and development arises through specific experiences along features dimensions, then less-familiar colors should be lower in capacity than familiar colors and more comparable to capacity for shapes.

Experiment 2a method

Participants Twenty 7-year-olds (*M* age = 7.38 years, *SD* = 3.42 months, 8 girls and 12 boys) participated in this experiment. Two additional children participated but were excluded from analyses, one due to equipment failure, and one due to a cognitive impairment that made completing the task too difficult.

Apparatus The stimuli and apparatus were identical to those described in Experiment 1 (see Fig. 3A for shapes, 3B for colors).

Procedure The procedure was identical to that described in Experiment 1 with two exceptions. First, children were informed that they would be completing two memory games, one with colors and one with shapes. The order of features was counter-balanced across participants, and all trials for one feature were completed before beginning the trials for the other feature. Second, we did not include test trials for set sizes one and two. Instead, children completed the practice block (with set sizes one and two, as in Experiment 1), then completed test trials for set size three, four, and five, in that order. Because the K_{max} estimates

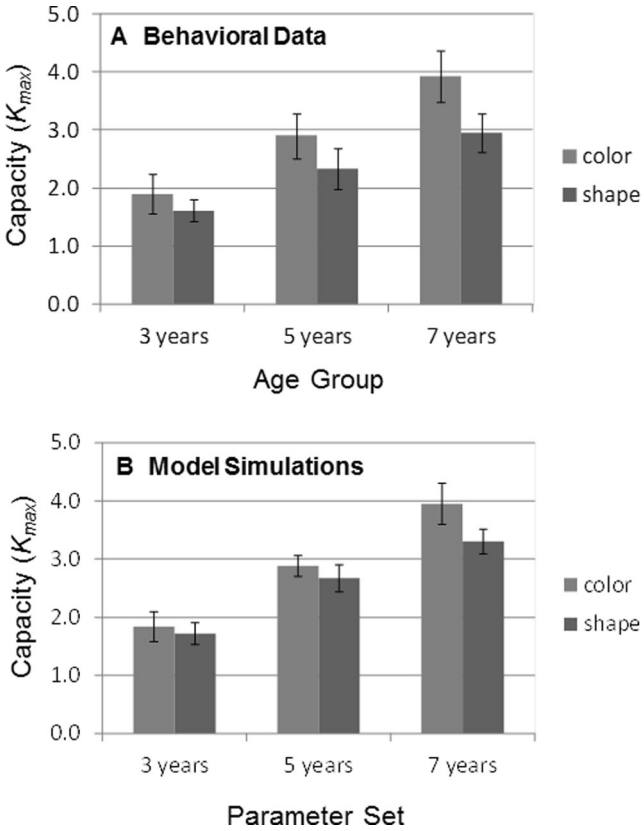

Fig. 6 (**A**) Mean capacity estimates across age groups and feature types for Experiment 1 (shape) with results from Simmering (2012) for comparison (color). (**B**) Mean capacity estimates derived from simulations of the DFT for parameters tuned to be weaker for shape than color. Error bars show 95 % confidence intervals

derived for 7-year-olds in Experiment 1 and Simmering (2012) all came from set sizes three or higher, we did not need to include test trials at the smaller set sizes. Reducing the number of set sizes tested also kept the total duration of the session within reason for child participants, under 30 min.

Experiment 2a results and discussion

Participants' responses were again classified as correct rejections, hits, misses, and false alarms, separately for each set size and feature type. Figure 7 shows the distribution of these response types; recall that correct rejections and false alarms sum to 1.0 (no-change trials) and hits and misses sum to 1.0 (change trials). As this figure shows, correct rejection and hits (i.e., correct responses) were most common, especially at lower set sizes; as set size increased, errors increased, especially misses. Furthermore, errors were more prevalent on shape versus color trials.

As in Experiment 1, we computed a K_{max} estimate for each participant, separately for each feature; mean K_{max} estimates were 3.54 (SD = 0.90) for color and 2.88 (SD = 0.65) for shape. A two-tailed paired-sample t-test on K_{max} estimates revealed that color capacity was significantly higher than shape capacity, t_{19} = 2.56, p = .019, d = 0.58, replicating the comparison between Experiment 1 and Simmering (2012).

Across Experiments 1 and 2a, results showed that children's capacity estimates were higher for colors than shapes. As explained in the introduction, the DFT could capture these results through memory for shapes that is relatively less mature than memory for colors. A further implication of this developmental change is that the advantage for color arises through more experience with colors than with shapes. As an initial test of this possibility, in Experiment 2b we compared children's memory for less-familiar colors to their memory for shapes.

Experiment 2b method

Participants Twenty 7-year-olds (M age = 7.58 years, SD = 6.36 months, 10 girls and 10 boys) participated in this experiment. Two additional children participated but were excluded from analyses due to incomplete data.

Apparatus The apparatus was identical to that described in Experiments 1 and 2a, as were the shape stimuli (see Fig. 2A); for color stimuli, unfamiliar colors were selected by modifying the RBG values to intermediate values along one dimension (see Fig. 3C for unfamiliar colors, and Appendix for RGB values).

Procedure The procedure was identical to that described in Experiment 2a.

Experiment 2b results and discussion

Participants' responses were again classified as correct rejections, hits, misses, and false alarms, separately for each set size and feature type. Figure 7 shows the distribution of these response types; recall that correct rejections and false alarms sum to 1.0 (no-change trials) and hits and misses sum to 1.0 (change trials). As this figure shows, correct rejection and hits (i.e., correct responses) were most common, especially at lower set sizes; as set size increased, errors increased, especially misses. Furthermore, errors were more comparable across shape and color trials, relative to Experiment 2a.

As in Experiments 1 and 2a, we computed a K_{max} estimate for each participant, separately for each feature; mean K_{max} estimates were 2.89 (SD = 1.04) for unfamiliar colors and 2.76 (SD = 0.83) for shapes. A two-tailed paired-sample t-test on K_{max} estimates revealed no difference (t_{19} = 0.49, p = .630), as predicted. We next compared capacity for unfamiliar colors (from the current experiment) to capacity for familiar colors (from Experiments 2a) and found that capacity was significantly lower for unfamiliar colors, t_{38} = 2.09, p = .043, d =

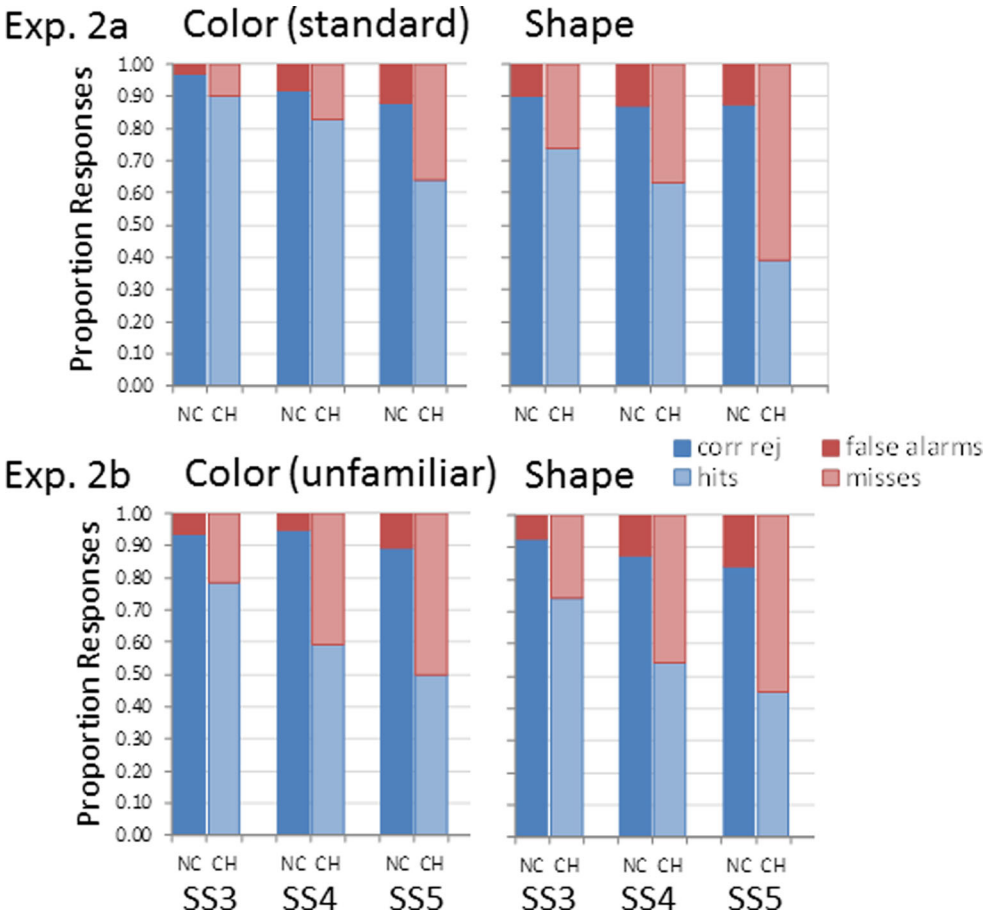

Fig. 7 Proportions of response types across set sizes and feature types for Experiment 2. Corr rej = correct rejections; SS = set size; NC = no-change trials; CH = change trials

0.66. Thus, as predicted, capacity for unfamiliar colors was similar to capacity for shapes, and both were lower than capacity for the canonical colors tested in change detection. Although these results are consistent with our predictions, more controlled experiments will be needed to test this account more rigorously (discussed further below).

General discussion

The goal of these experiments was to test how VWM differs across feature types over development. According to the DFT, capacity increases through the strengthening of neural connectivity underlying representation of visual features (Perone et al., 2011; Simmering, 2008; Simmering & Patterson, 2012; Simmering & Schutte, in press). If this change in connectivity arises through experience (cf. Perone & Spencer, 2013a), then features that are more common or familiar should improve more quickly over development. Experiment 1 showed that older children had higher capacity for colors than shapes. In Experiment 2a, we replicated this finding within a single group of 7-year-olds and in Experiment 2b showed that it was specific to common colors; capacity for unfamiliar colors was lower than capacity for familiar colors and comparable to capacity for shapes. Taken together, these results support the DFT account of developmental changes in capacity limits. Below we compare this account to other theories of VWM and working memory more generally, then discuss the theoretical motivation for how development is implemented in the DFT, as well as additional consequences in the model. We conclude by discussing limitations of the model and the long-term goals of this research program.

Before considering these theoretical implications of our findings, it is important to note potential alternative explanations for these effects. First, the stimuli we chose to use as less-familiar colors were not precisely matched to the standard colors in terms of discriminability; it is possible that our changes in the RGB values resulted in colors that were more similar to one another, which drove our effect. This is not necessarily inconsistent with the DFT account: Simmering and Patterson (2012) showed developmental improvements in discrimination thresholds for colors, which purportedly arise through the same mechanism described here. This would suggest that less-familiar colors could also be more difficult to discriminate, even with comparable sensory changes. Simmering and Patterson avoided the potential confound of

different sensory properties across colors by comparing the same colors between age groups; we cannot be sure there were equivalent sensory differences among the colors within our two stimulus sets.

Another possible explanation for our findings is that all of the standard colors were easy to name, whereas some of the shapes and less-familiar colors were not (see Fig. 3), and that performance was better for stimuli that were easier to name. However, prior research suggests this is unlikely, as children 7 years and younger do not spontaneously verbally recode visual stimuli (Pickering, 2001). Furthermore, with set sizes of at least three items and only 500 ms to encode, as in Experiment 2, it is doubtful that children would have had sufficient time to benefit from naming the colors in the displays of familiar colors (due to generally slower naming in children; cf. Case, Kurland, & Goldberg, 1982). Given these potential alternative explanations, further studies will be needed to definitively support the role of experience to the exclusion of other potential explanations. Nonetheless, these results provide preliminary support for the DFT account of developmental change in VWM through experience.

Comparisons to other theories of working memory

Could slot or resource theories also account for our findings? As reviewed above, most slot models do not specify the manner by which the number of slots increases, providing no opportunity for comparison. One account has suggested that slots arise through synchronously firing neural assemblies (Vogel et al., 2001), and developmental increases in the number of slots could arise through improvements in synchronization (Riggs et al., 2011). However, the role of experience versus maturation in these purported changes in synchronization has not been explored, especially with regard to how neural synchrony could support VWM (Uhlhaas, Roux, Rodriguez, Rotarska-Jagiela, & Singer, 2010). It is possible that the consequences of increased neural synchrony could be simulated as stronger connections within the DFT, suggesting potential convergence between these proposed mechanisms. Further computational and empirical work will be needed to test this possibility.

From a resource perspective, Bays et al. (2011) showed independence of errors along different feature dimensions (color and orientation) of the same objects. Although they did not explicitly compare resolution across feature types, their proposal that the features are represented by independent pools of resources suggests their theory could account for capacity differences across feature types. Regarding developmental change, Burnett Heyes et al. (2012) argued that developmental improvements in resolution could result from "sharpening" of representations within neural populations, which is consistent with the developmental mechanism in the DFT. However, Burnett Heyes et al. did not specify the source of this developmental change (e.g., through specific experience versus general maturation) so it is unclear whether this account would predict our results from Experiment 2b.

Beyond slot and resource accounts of VWM development, we consider a few more general theories of working memory development in comparison to the DFT. Many of these theories are tied closely to the tasks they were developed to explain, such as complex tasks that require alternating between processing and storage across trials. For example, the counting span task includes a series of displays with different numbers of dots; the participant's task is to count the dots in each display and remember the number of dots across displays to report at the end (e.g., Towse & Hitch, 1995). Theories of tasks like these attribute most developmental change to improvements in processes specific to these tasks, including rehearsal, task-switching, and processing speed (e.g., Barrouillet & Camos, 2007; Case, 1995; Towse & Hitch, 1995). It is unclear how such theories could be adapted to explain developmental improvements in simpler tasks, such as the change detection task used here, which minimizes demands on more complex processes (see Simmering & Perone, 2013, for discussion).

As noted above, the DFT account of developmental change through experience is similar to knowledge accounts of growth in verbal working memory capacity. For example, Case et al. (1982) showed that developmental differences in recall could be eliminated by providing more familiar stimuli to children and unfamiliar stimuli to adults (but see Cowan, Ricker, Clark, Hinrichs, & Glass, 2014, for evidence that knowledge cannot fully explain development in visual recognition of letters versus unfamiliar characters). Chi (1978) also showed that 8- to 10-year-old chess experts outperformed adult chess novices when stimuli were comprised of meaningful chess configurations, but performed worse on more typical stimuli (i.e., digit span). Although these results are similar to one another, the theoretical explanations differ. Chi's results have been attributed to experts "chunking" chess pieces into meaningful units based on their experience (Chi, 1978). Case et al. (1982) quantified the effect of knowledge by equating the amount of time it took children to repeat familiar words with the time it took adults to repeat unfamiliar (nonsense) words. Case et al. viewed repetition time as reflecting "operating efficiency", which improves over development through experience. In this way, Case et al.'s account is similar to the strengthening of connectivity in the DFT: the more a given stimulus is experienced, the more efficiently it is processed. In addition to increases in capacity and resolution, stronger connections in the DFT lead to faster build-time for peaks (Simmering, 2015), which could be analogous to the operating efficiency described by Case et al. This comparison highlights an important difference between the DFT and other theories of working memory and development: by

implementing tasks within a process-based model, we can test multiple consequences of a single developmental mechanism and synthesize many findings within a single theoretical framework.

Development in the DFT

In this section we first describe more specific details of the choices for how to implement development in the model, then discuss additional consequences of these changes. To simulate developmental change from 3 to 7 years in the DFT, we varied the strength of three parameters: the stimulus input, the strength of excitatory connections within the working memory field, and the strength of inhibitory connections from the inhibitory layer to the working memory field. These latter two parameters jointly comprise the interaction function within the working memory field, with stronger connections producing more robust working memory representations (see Simmering, 2015; Simmering & Schutte, in press, for further discussion). The change in input strength would correspond to stronger projections from earlier visual areas. These types of developmental changes have been shown previously to capture improvements in infant visual memory (Perone et al., 2011; Perone & Spencer, 2013b, 2014) and spatial cognition during early childhood (see Simmering & Schutte, in press, for review) using related DFT architectures.

One question that arises from the implementation of development in a dynamic neural field model is whether these results can be connected to changes in the brain during early childhood. Although the DFT modeling framework was built from neural principles (see Schneegans, Lins, & Schoner, in press, for review), these recent expansions into visuospatial cognition are not directly linked to specific neural structures. However, there are potential parallels between the types of development implemented in the model and neural development such as changes in myelination, synaptic density, synchrony, and/or long-term potentiation. The strengthening of connections within the DFT could be capturing the consequences of one or more of these underlying neural changes. Regardless of the specific neural change that underlies developmental improvements in VWM, a computational model like the DFT can provide a useful tool in understanding how behavioral changes relate to these types of neural changes.

Lastly, we consider additional consequences arising from these developmental changes in the DFT. Simmering (2015) explored a range of changes in VWM functioning by simulating children's performance in two VWM tasks, the change detection task and an infant preferential looking paradigm designed to estimate capacity (Ross-Sheehy, Oakes, & Luck, 2003). By fitting performance in both tasks over development, model simulations illustrated eight consequences of strengthening connectivity in VWM: (1) stronger representations; (2) faster encoding; (3) more resistance to interference and (4) decay; (5) increased capacity and (6) resolution; (7) better correspondence between memory and behavior across tasks; and (8) reduced effects of task context on memory. Simmering referred to these collectively as developmental increases in "real-time stability," that is, improved robustness with which the VWM system can be used in service of different tasks over development. She argued that previous theories of working memory development that have proposed some of these sources in isolation, or even opposition to each other, could be synthesized into a single, general mechanism for developmental change.

Outlook

There remain a number of challenges in applying the DFT to VWM performance and development. One notable limitation, discussed further by Simmering (2015), is that the current model architecture represents only a single feature dimension, not the locations of these features in space, or the binding of features together. Evidence suggests that infants achieve the ability to bind colors to locations within the first year (e.g., Oakes, Ross-Sheehy, & Luck, 2006), but relatively little is known about how feature binding changes during early childhood. Within the DFT framework, an expanded architecture has been developed that could bind features together via their shared spatial locations. In particular, Schneegans, Spencer, and Schöner (in press) proposed that parallel one-dimensional representations of color, shape, and location could be linked through two-dimensional (e.g., color-space) fields. They demonstrated that this architecture could not only detect changes to new features (similar to change detection model presented here) but also changes in the bindings of features between objects (by virtue of the new feature-location binding). Their simulations thus far have only been used to demonstrate how such binding could occur, but the expanded architecture has not been tested quantitatively to see if it could produce the patterns of results shown in behavioral tasks.

The broader goal of this line of research is to develop a more comprehensive theory of VWM, encompassing not only limitations in capacity and resolution, but also the source of developmental improvements in each of these and how they relate to other developmental changes (Simmering, 2015). The behavioral and computational results presented here provide support for the DFT as an alternative to slot and resource explanations of VWM capacity, and initial evidence for the role of experience in capacity increases. A complete understanding of VWM requires moving beyond a focus on representation to consider the processes that transform representations

into behavioral output, and explaining how these abilities develop into the adult form that has been the primary emphasis in previous research.

Acknowledgments Thanks to the families who participated in this research and the research assistants who aided in data collection. Participant recruitment and programming was funded by the Eunice Kennedy Shriver National Institute of Child Health & Human Development of the National Institutes of Health (R03-HD067481) and the Waisman Intellectual and Developmental Disabilities Research Center grant (P30HD03352). The content is solely the responsibility of the authors and does not necessarily represent the official views of the National Institutes of Health. Thanks to Rob Olson for programming assistance and to John P. Spencer for input during the conceptualization and writing of the manuscript. A subset of the data included here was presented at the 70th biennial meeting of the Society for Research in Child Development in Seattle, Washington.

Appendix

Model parameters and equations

This section describes the equations that govern activation in the five fields of the unified model used in the present report. The three-layer model described by Johnson et al. (2014) consists of an excitatory field, *u(x;t)*, which receives afferent sensory input, *S(x;t)*; a shared inhibitory field, *v(x;t)*; and second excitatory field, *w(x;t)* that receives excitatory input, primarily from the first excitatory field but also a weak copy of the sensory input. These excitatory fields were connected to response nodes *d* and *s*, indicating *different* and *same* responses in the change detection task; activation to these nodes was controlled by a gate node, *g*, following Simmering (2008, 2015)

Contrast field Activation in the contrast field, CF(*u*), is captured by:

$$\tau_u \dot{u}(x,t) = -u(x,t) + h_u + uStim(x,t) + \int c_{uu}(x-x')\Lambda_{uu}(u(x',t))dx' - \int c_{uv}(x-x')\Lambda_{uv}(v(x',t))dx', t + \int c_{uH}(x,x')H_u(x,t)dx' + [a_{ud}\Lambda_{ud}(r_d(t)) + (c_{ud} * r_d)] + noise.$$

Table 1 Parameter values fitting adults' performance

Field/nodes	τ	Resting level	Self-excitation	Excitatory projection(s)	Inhibitory projection(s)	Input	Noise
CF(*u*)	$\tau_u = 80$ $\tau_{qh} = 50$[b]	$h_u = -6.75$[a]	$c_{uu} = 2$ $\sigma_{uu} = 3$	$c_{uH} = 0.2$[b] $\sigma_{uH} = 6.4$[b] $c_{ud} = 1$[d] $c_{uf} = 1$[d]	$c_{uv} = 1.85$ $\sigma_{uv} = 26$ $k_{uv} = 0.05$[d]	$c_{ustim} = 30$[c] $\sigma_{ustim} = 3$	$q_u = 0.04$[b] $\sigma_q = 1$[b] $q_h = 6$[b]
Inhib(*v*)	$\tau_v = 10$	$h_v = -12$[a]		$c_{vu} = 2$ $\sigma_{vu} = 10$ $c_{vw} = 1.95$ $\sigma_{vw} = 5$			
WM(*w*)	$\tau_w = 80$	$h_w = -4.5$[a]	$c_{ww} = 3.15$ $\sigma_{ww} = 3$	$c_{wu} = 1.6$ $\sigma_{wu} = 5$ $c_{wd} = 1$[d]	$c_{wv} = 0.325$ $\sigma_{wv} = 42$ $k_{wv} = 0.08$[d]		
Hebb. (*H*)	$\tau_{Hbuild} = 3000$[b] $\tau_{Hdecay} = 100{,}000$[b]						
Resp. (*R*)	$\tau_R = 80$		$c_{RR} = 1.85$	$c_{Rg} = 4.25$	$c_{R-} = 14$		$q_R = 0.065$
Diff. (*d*)	$h_d = -5$		$c_{du} = 1.4$				
Same (*s*)	$h_s = -4.75$		$c_{sw} = 0.275$				
Gate (*g*)	$\tau_g = 80$	$h_g = -4.92$	$c_{gg} = 4.8$	$c_{gw} = 0.03$		$c_{gstim} = 0.03$ $c_{gT} = 18$	$q_g = 0.025$

Note. Following mathematical convention, parameter subscripts indicate the field receiving the projection followed by the field/node sending the projection (i.e., c_{wu} indicates the strength of a projection into *w*/working memory from *u*/contrast field). Parameters shown in the Response (Resp.) row were identical for the Same and Different (Diff.) nodes; any parameters that differed between these nodes are shown in the following rows

[a] The resting levels of these three fields also included colored noise; the equation for these resting levels contains two parameters, q_h and τ_{qh}

[b] These parameters were identical across fields, and are reported only once in the table for simplicity

[c] Input also projected weakly into *w*/working memory (strength scaled by 0.2)

[d] These projections were applied uniformly across the fields, thus there are no corresponding σ values

where $\dot{u}(x,t)$ is the rate of change of the activation level for each node across the spatial dimension, x, as a function of time, t. The constant τ_u determines the time scale of the dynamics (Erlhagen & Schöner, 2002). The first factor that contributes to the rate of change of activation in CF(u) is the current activation in the field, $-u(x,t)$, at each site x. This component is negative so that activation changes in the direction of the resting level h_u. The resting level included colored noise, which was determined by the equation $\tau_h\,(t) = -h(t) + q_h * noise$, in which the current resting state is increased or decreased by a random amount (q_h* $noise$) at each time step. This is termed colored noise because the value at each time step is partially determined by the value at the previous time step; this contrasts with white noise, which is independent across time steps.

Inputs to the model take the form of a Gaussian distribution, $uStim(x,t) = c\exp[-(x-x_{center})\ \frac{2}{2\sigma^2]\chi^{(t)}}$, with the positions of colors centered at x_{center}, input widths of σ, and strengths c. These inputs are turned on and off through time as items appear and then disappear in the display. This time interval is specified by the pulse function $\chi^{(t)}$. Activation in CF(u) is also influenced by the local excitation-lateral inhibition interaction profile, defined by self-excitatory projections, $\int c_{uu}(x-x')\Lambda_{uu}(u(x',t))dx'$, and inhibitory projections from Inhib(v), $\int c_{uv}(x-x')\Lambda_{uv}(v(x',t))dx'$. These interactions are specified by the convolution of a Gaussian kernel with a sigmoidal threshold function. In particular, the Gaussian kernel was defined as $c(x-x') = c\ \exp[-(x-x')\ \frac{2}{2\sigma^2}] - k$, where the σ determines the neighboring nodes across which interactions propagate, c determines the strength, and k sets the resting level. Note that k was set to 0 for all excitatory convolutions. Only nodes with above-threshold activation (i.e., above 0) participate in interactions, as determined by a sigmoidal function, $\Lambda(u) = \frac{1}{1+\exp[-\beta u]}$, where β is the slope of the sigmoid, that is, the degree to which nodes close to threshold (i.e., 0) contribute to the activation dynamics. Lower slope values permit graded activation near threshold to influence performance, while higher slope values ensure that only above-threshold activation contributes to the activation dynamics. At extreme slope values, the sigmoid function approaches a step function. For all simulations presented here, $\beta = 0.5$.

Activation in CF(u) is influenced by input from the corresponding Hebbian field $H_{CF}(u_H)$, as defined by $\int c_{uH}(x,x')H_u(x,t)dx'$ (see below for u_H equation). This input is determined by the convolution of a Gaussian projection, $c_{uH}(x,x')$, which determines the neighborhood of nodes across which Hebbian traces have an influence, and the strength of the trace within the Hebbian field, $H_u(x,t)$. Next, a global input to CF(u) is projected from the *different* response node (r_d) when the activation of one of these nodes is above zero.

Lastly, activation within the field is influenced by the addition of a stochastic component consisting of spatially correlated noise, $noise = q\int dx' g_{noise}(x-x')\xi(x',t)$. Noise was added to the simulations by convolving a noise field composed of independent noise sources with a Gaussian kernel specified by: $g_{noise}(x-x') = \frac{1}{\sqrt{2\sigma_{noise}}}\exp[-(x-x')\ \frac{2}{2\sigma_{noise}{}^2]}$, where σ_{noise} is the spatial spread of the noise kernel (set to 10 in all simulations). For discussion of the differences between spatially correlated noise and Gaussian white noise, see Schutte, Spencer, & Schöner (2003).

Inhibitory field The second field of the model, Inhib(v), is specified by the following equation:

$$\tau_v \dot{v}(x,t) = -v(x,t) + h_v + \int c_{vu}(x-x')\Lambda_{vu}(u(x',t))dx' + \int c_{vw}(x-x')\Lambda_{vw}(w(x',t))dx' + noise.$$

As before, $\dot{v}(x,t)$ specifies the rate of change of activation across the population of feature-selective nodes, x, as a function of time, t; the constant τ sets the time scale (note that the time scale for inhibition is faster than for the excitatory fields, i.e., $\tau_v < \tau_u$); $v(x,t)$ captures the current activation of the field; and h_v sets the resting level of nodes in the field. As with CF(u), colored noise was added to the resting level. Inhib(v) receives activation from two projections: one from CF(u), $\int c_{vu}(x-x')\Lambda_{vu}(u(x',t))dx'$; and one from WM($w$), $\int c_{vw}(x-x')\Lambda_{vw}(w(x',t))dx'$.

As described above, these projections are defined by the convolution of a Gaussian kernel with a sigmoidal threshold function. Finally, this field also receives spatially-correlated noise, as described above. This noise is independent from the noise sources in the other fields of the model.

Working memory field The third field of the model, WM(w), is governed by the following equation:

$$\tau\ \dot{w}(x,t) = -w(x,t) + h_w + wStim(x,t) + \int c_{ww}(x-x')\Lambda_{ww}(w(x',t))dx' - \int c_{wv}(x-x')\Lambda_{wv}(v(x',t))dx' + \int c_{wu}(x-x')\Lambda_{wu}(u(x',t))dx' + \int c_{wH}(x,x')H_w(x,t)dx' + [a_{ws}\Lambda_{ws}(r_s(t)) + (c_{ws}*r_s)] + noise.$$

As in the previous equations, (x,t) is the rate of change of activation across the population of spatially tuned nodes, x, as a function of time, t; the constant τ sets the time scale; $w(x,t)$ captures the current activation of the field; and h_w sets the resting level. As with CF(u), colored noise was added to the resting level. This field also receives direct target inputs, w$Stim(x,t)$, although the strength of this input is weaker (strength scaled by 0.2) than the direct input to CF(u). As with CF(u), this input turns on and off over time to correspond to the task structure.

Table 2 Parameter values fitting children's performance for colors

Field/node	τ	Resting level	Self excitation	Excitatory projection(s)	Inhibitory projection(s)	Input	Noise
CF(u)			c_{uu3} = 1.7 c_{uu5} = 1.7 c_{uu7} = 1.82		c_{uv} = 0.6475 k_{uv3} = 0.0375 k_{uv5} = 0.0375 k_{uv7} = 0.045	c_{ustim3}= 9.0[a] c_{ustim5}= 10.65[a] c_{ustim7}= 14.1[a] σ_{ustim} = 4.5	q_u = 0.05[b]
WM(w)			c_{ww3}= 1.2285 c_{ww5}= 1.6695 c_{ww7}= 2.583		c_{wv3}= 0.17225 c_{wv5}= 0.2015 c_{wv7}= 0.21125 k_{wv3} = 0.06 k_{wv5} = 0.06 k_{wv7} = 0.072		
Hebb. (H)	$\tau_{Hbuild3}$ = 750[b] $\tau_{Hbuild5}$ = 2250[b] $\tau_{Hbuild7}$ = 3000[b] τ_{Hdecay} = 150,000[b]						
Resp. (R)			c_{RR} = 1. 3875		c_{R-} = 10.5		q_R = 0.0813
Diff. (d)			c_{du3} = 0.75 c_{du5} = 1.246 c_{du7} = 1.4				
Same (s)	h_s = -4.5		c_{sw} = 0.01815				
Gate (g)				c_{gw} = 0.05			

Note. Only parameter values that differ from those fitting adults' performance (reported in Table 1) are shown here for simplicity. These parameters were tuned to fit behavioral data reported by Simmering (2012). Underlined parameter values were tuned to fit 5-year-olds' performance on shapes, then modified by the same proportion (strength scaled by 0.97) to predict 3- and 7-year-olds' capacity for shapes

[a] Input also projected weakly into w/working memory (strength scaled by 0.2)

[b] These parameters were identical across fields, and are reported only once in the table for simplicity

Table 3 Model fits of 5-year-olds' performance on color and shape conditions in change detection

	Behavioral data		Simulations	
	CR rate	H rate	CR rate	H rate
Color SS1	.92 (.11)	.96 (.09)	.95 (.11)	.93 (.10)
Color SS2	.93 (.11)	.89 (.16)	.94 (.08)	.91 (.09)
Color SS3	.89 (.14)	.74 (.22)	.89 (.12)	.76 (.19)
Color SS4	.88 (.15)	.62 (.24)	.88 (.14)	.60 (.16)
Color SS5	.79 (.24)	.54 (.25)	.60 (.23)	.48 (.16)
Shape SS1	.93 (.09)	.99 (.04)	.92 (.10)	.95 (.10)
Shape SS2	.90 (.11)	.86 (.14)	.99 (.04)	.84 (.14)
Shape SS3	.87 (.18)	.55 (.19)	.86 (.14)	.78 (.18)
Shape SS4	.83 (.17)	.52 (.23)	.83 (.14)	.65 (.17)
Shape SS5	.88 (.16)	.35 (.18)	.70 (.18)	.41 (.18)

Note. The behavioral means from the color condition included the 28 children from the standard and "card" versions reported by Simmering (2012); the shape condition included the 14 children reported in Simmering (2008, 2015) Experiment 3. Each set of simulations included 20 runs of the model (equivalent to 20 participants). Standard deviations (across participants for behavioral data, across runs for simulations) are shown in parentheses. Mean absolute error between the behavioral data and simulations was .05 for color and .08 for shape. CR = correct rejections, H = hits

Table 4 Model fits of 3- and 7-year-olds' performance on color change detection

	Behavioral data		Simulations	
	CR rate	H rate	CR rate	H rate
3y SS1	.88 (.19)	.88 (.14)	.94 (.08)	.83 (.14)
3y SS2	.85 (.18)	.83 (.16)	.88 (.12)	.72 (.15)
3y SS3	.77 (.27)	.64 (.27)	.75 (.18)	.63 (.23)
7y SS1	.99 (.03)	.99 (.03)	.97 (.07)	.99 (.04)
7y SS2	1.00 (.03)	.98 (.08)	.97 (.07)	.93 (.11)
7y SS3	.90 (.17)	.92 (.12)	.95 (.08)	.85 (.16)
7y SS4	.91 (.12)	.77 (.19)	.84 (.17)	.74 (.19)
7y SS5	.88 (.21)	.69 (.23)	.67 (.19)	.82 (.17)

Note. The behavioral means for 3-year-olds (3y) included the 14 children from Simmering (2012); means for 7-year-old (7y) included the 28 children from the standard and "card" versions reported by Simmering (2012). Each set of simulations included 20 runs of the model (equivalent to 20 participants). Standard deviations (across participants for behavioral data, across runs for simulations) are shown in parentheses. Mean absolute error between the behavioral data and simulations was .05 for 3-year-olds and .07 for 7-year-olds. CR = correct rejections, H = hits

Table 5 RGB values for color stimuli in experiments 2a (standard) and 2b (unfamiliar)

Standard colors	R	G	B	Unfamiliar colors	R	G	B
Black	0	0	0	Brown	51	51	0
Blue	0	0	255	Blue/green	0	128	128
Cyan	0	255	255	Lime	155	255	89
Green	0	255	0	Sea foam green	0	255	128
Red	255	0	0	Maroon	128	0	0
Violet	238	130	238	Magenta	204	0	153
White	255	255	255	Salmon	255	128	64
Yellow	255	255	0	Mustard	128	128	0

WM(w) also receives self-excitation, $\int c_{ww}(x-x')\Lambda_{ww}(w(x',t))dx'$, lateral inhibition from Inhib(v), $\int c_{wv}(x-x')\Lambda_{wv}(v(x',t))dx'$, excitatory input from CF(u), $\int c_{wu}(x-x')\Lambda_{wu}(u(x',t))dx'$, and excitatory input from the corresponding Hebbian field $H_{WM}(w_H)$. Next, a global input to WM(w) is projected from the *same* response node (r_s) when the activation of this node is above zero. Finally, this field also receives spatially-correlated noise, as described above. Again, this noise is independent from the noise sources in the other fields of the model.

Hebbian fields Activation in the Hebbian fields, $H_{CF}(u_H)$ and $H_{WM}(w_H)$, was governed by the states of the associated excitatory field (for simplicity, only the $H_{PF}(u_H)$ equation is shown, as the $H_{WM}(w_H)$ equation is analogous):

$$\tau_{ltm}\ \dot{u}_{ltm}(x,t) = \dot{u}_{ltmbuild}(x,t) + \dot{u}_{ltmdecay}(x,t)$$

The rate of change of activation, $\dot{u}_{ltm}(x,t)$, for each node in the Hebbian field across the spatial dimension, x, as a function of time, t, is specified by two components: the build-up of activation, $\dot{u}_{ltmbuild}$, and the decay of activation, $\dot{u}_{ltmdecay}$. These components were specified as follows:

$$\tau_{ltmbuild}\dot{u}_{ltmbuild}(x,t) = [u_{ltm}(x,t) + \Lambda(u(x,t)]\cdot\theta(u(x,t));$$
$$\tau_{ltmdecay}\dot{u}_{ltmdecay}(x,t) = u_{ltm}(x,t)\cdot[1-\theta(u(x,t))]\ .$$

The shunting function θ ($\theta = 1$ if $u(x,t) > 0$ and $\theta = 0$ otherwise) determines where the activation is built up and maintained in u_H. The build-up rate is relatively fast while the decay rate is much slower; this allows previous memory to be maintained over longer periods. Separating the build-up and decay mechanisms approximates accumulation and depression of synaptic change (Deco & Rolls, 2005).

Details of unfamiliar color stimuli for Experiment 2b

To create eight color stimuli for Experiment 2b that were of similar discriminability to the canonical colors used in Experiment 2a and most studies in the field (e.g., Simmering, 2012), we took the list of RGB values (shown in Table 5) and changed one of the dimensions by values of approximately 127 or 51. This changed the value along that dimension to roughly half or one-third of its previous value.

References

Alvarez, G. A., & Cavanagh, P. (2004). The capacity of visual short-term memory is set both by visual information load and by number of objects. *Psychological Science, 15*(2), 106–111.

Awh, E. S., Barton, B., & Vogel, E. K. (2007). Visual working memory represents a fixed number of items regardless of complexity. *Psychological Science, 18*(7), 622–628.

Barrouillet, P., & Camos, V. (2007). The time-based resource-sharing model of working memory. In N. Osaka, R. H. Logie, & M. D'Esposito (Eds.), *The Cogntive neuroscience of working memory: Behavioural & neural correlates*. Oxford University Press.

Bays, P. M., & Husain, M. (2008). Dynamic shifts of limited working memory resources in human vision. *Science, 321,* 851–854.

Bays, P. M., Wu, E. Y., & Husain, M. (2011). Storage and binding of object features in visual working memory. *Neuropsychologia, 49,* 1622–1631.

Brainard, D. H. (1997). The psychophysics toolbox. *Spatial Vision, 10,* 433–436.

Burnett Heyes, S., Zokaei, N., van der Staaij, I., Bays, P. M., & Husain, M. (2012). Development of visual working memory precision in childhood. *Developmental Science, 15*(4), 528–539.

Case, R. (1995). Capacity based explanations of working memory growth: A brief history and a reevaluation. In F. M. Weinert & W. Schneider (Eds.), *Memory performance and competencies: Issues in growth and development* (pp. 23–44). Mahwah, NJ: Erlbaum.

Case, R., Kurland, M., & Goldberg, J. (1982). Operational efficiency and the growth of short-term memory span. *Journal of Experimental Child Psychology, 33,* 386–404.

Chi, M. T. H. (1978). Knowledge structure and memory development. In R. Siegler (Ed.), *Children's thinking: What develops? Thirteenth Annual Carnegie Symposium on Cognition*. Hillsdale, NJ: Erlbaum.

Cowan, N. (2001). The magical number 4 in short-term memory: A reconsideration of mental storage capacity. *Behavioral and Brain Sciences, 24,* 87–185.

Cowan, N., AuBuchon, A. M., Gilchrist, A. L., Ricker, T. J., & Saults, J. S. (2011). Age differences in visual working memory capacity: not based on encoding limitations. *Developmental Science, 14,* 1066–1074. doi:10.1111/j.1467-7687.2011.01060.x

Cowan, N., Elliott, E. M., Saults, J. S., Morey, C. C., Mattox, S., Hismjatullina, A., & Conway, A. R. A. (2005). On the capacity of attention: Its estimation and its role in working memory and cognitive aptitudes. *Cognitive Psychology, 51,* 42–100.

Cowan, N., Morey, C. C., Chen, Z., Gilchrist, A. L., & Saults, J. S. (2008). Theory and measurement of working memory capacity limits. In *The psychology of learning and motivation* (Vol. 49, pp. 49–104). Elsevier.

Cowan, N., Ricker, T. J., Clark, K. M., Hinrichs, G. A., & Glass, B. A. (2014). Knowledge cannot explain the developmental growth of working memory capacity. *Developmental Science*. doi:10.1111/desc.12197

Edin, F., Klingberg, T., Johansson, P., McNab, F., Tegnér, J., & Compte, A. (2009). Mechanism for top-down control of working memory capacity. *Proceedings of the National Academy of Sciences, 106*(16), 6802–6807.

Hitch, G. J., Woodin, M. E., & Baker, S. (1989). Visual and phonological components of working memory in children. *Memory & Cognition, 17*(2), 175–185.

Johnson, J. S., & Simmering, V. R. (in press). Integrating perception and working memory in a three-layer dynamic field architecture. In G. Schöner, J. P. Spencer, & the DFT Research Group (Eds.), *Dynamic thinking: A primer on dynamic field theory*. New York, NY: Oxford University Press.

Johnson, J. S., Simmering, V. R., & Buss, A. T. (2014). Beyond slots and resources: Grounding cognitive concepts in neural dynamics. *Attention, Perception, & Psychophysics, 76*(6), 1630–1654. doi:10.3758/s13414-013-0596-9

Karatekin, C., & Asarnow, R. F. (1998). Working memory in childhood-onset schizophrenia and attention-deficit/hyperactivity disorder. *Psychiatry Research, 80,* 165–176.

Kleiner, M., Brainard, D. H., & Pelli, D. G. (2007). What's new in psychtoolbox-3? *Perception 36 ECVP Abstract Supplement*.

Luciana, M., Lindeke, L., Georgieff, M., Mills, M., & Nelson, C. A. (1999). Neurobehavioral evidence for working-memory deficits in school-aged children with histories of prematurity. *Developmental Medicine & Child Neurology, 41*(8), 521–533.

Miles, C., Morgan, M. J., Milne, A. B., & Morris, E. D. M. (1996). Developmental and individual differences in visual memory span. *Current Psychology, 15*(1), 53–67.

Miller, P. H. (2013). The history of memory development research: remembering our roots. In P. J. Bauer & R. Fivush (Eds.), *The Wiley handbook on the development of children's memory* (Vol. I/II, pp. 19–40). Chichester: Wiley and Sons.

Oakes, L. M., Ross-Sheehy, S., & Luck, S. J. (2006). Rapid development of feature binding in visual short-term memory. *Psychological Science, 17*(9), 781–787.

Olsson, H., & Poom, L. (2005). Visual memory needs categories. *Proceedings of the National Academy of Science U.S.A., 102*(24), 8776–8780.

Pashler, H. (1988). Familiarity and visual change detection. *Perception and Psychophysics, 44,* 369–378.

Pelli, D. G. (1997). The VideoToolbox software for visual psychophysics: Transforming numbers into movies. *Spatial Vision, 10,* 437–442.

Perone, S., Simmering, V. R., & Spencer, J. P. (2011). Stronger neural dynamics capture changes in infants' visual working memory capacity over development. *Developmental Science, 14,* 1379–1392. doi:10.1111/j.1467-7687.2011.01083.x

Perone, S., & Spencer, J. P. (2013a). Autonomous visual exploration creates developmental change in familiarity and novelty seeking behaviors. *Frontiers in Cognitive Science, 4,* 648. doi:10.3389/fpsyg.2013.00648

Perone, S., & Spencer, J. P. (2013b). Autonomy in action: Linking the act of looking to memory formation in infancy via dynamic neural fields. *Cognitive Science, 37,* 1–60. doi:10.1111/cogs.12010

Perone, S., & Spencer, J. P. (2014). The co-development of looking dynamics and discrimination performance. *Developmental Psychology, 50*(3), 837–852. doi:10.1037/a0034137

Pickering, S. J. (2001). The development of visuo-spatial working memory. *Memory, 9,* 423–432.

Raffone, A., & Wolters, G. (2001). A cortical mechanism for binding in visual working memory. *Journal of Cognitive Neuroscience, 13,* 766–785.

Riggs, K. J., McTaggart, J., Simpson, A., & Freeman, R. P. J. (2006). Changes in the capacity of visual working memory in 5- to 10-year-olds. *Journal of Experimental Child Psychology, 95,* 18–26.

Riggs, K. J., Simpson, A., & Potts, T. (2011). The development of visual short-term memory for multifeature items during middle childhood. *Journal of Experimental Child Psychology, 108,* 802–809.

Ross-Sheehy, S., Oakes, L. M., & Luck, S. J. (2003). The development of visual short-term memory capacity in infants. *Child Development, 74,* 1807–1822.

Schneegans, S., Lins, O. G., & Schoner, G. (in press). Dynamic field theory and ties to neurophysiology. In G. Schoner, J. P. Spencer, & the DFT Research Group (Eds.), *Dynamic thinking: A primer on dynamic field theory*. New York, NY: Oxford University Press.

Schneegans, S., Spencer, J. P., & Schöner, G. (in press). Integrating "what" and "where": Visual working memory for objects in a scene. In G. Schöner, J. P. Spencer, & the DFT Research Group (Eds.), *Dynamic thinking: A primer on dynamic field theory*. New York, NY: Oxford University Press.

Schutte, A. R., Spencer, J. P., & Schöner, G. (2003). Testing the dynamic field theory: Working memory for locations becomes more spatially precise over development. *Child Development, 74*(5), 1393–1417.

Shipstead, Z., Hicks, K. L., & Engle, R. W. (2012). Working memory training remains a work in progress. *Journal of Applied Research in Memory and Cognition, 1*(3), 217–219.

Simmering, V. R. (2008). *Developing a magic number: The dynamic field theory reveals why visual working memory capacity estimates differ across tasks and development* (Unpublished doctoral thesis). University of Iowa, Iowa City, IA.

Simmering, V. R. (2012). The development of visual working memory capacity in early childhood. *Journal of Experimental Child Psychology, 111,* 695–707.

Simmering, V. R. (2015). Working memory capacity in context: Modeling dynamic processes of behavior, memory, and development. *Manuscript under Review*.

Simmering, V. R., & Patterson, R. (2012). Models provide specificity: Testing a proposed mechanism of visual working memory capacity development. *Cognitive Development, 27*(4), 419–439. doi:10.1016/j.cogdev.2012.08.001

Simmering, V. R., & Perone, S. (2013). Working memory capacity as a dynamic process. *Frontiers in Developmental Psychology, 3,* 567. doi:10.3389/fpsyg.2012.00567

Simmering, V. R., & Schutte, A. R. (in press). Developmental dynamics: The spatial precision hypothesis. In G. Schöner, J. P. Spencer, & the DFT Research Group (Eds.), *Dynamic thinking: A primer on dynamic field theory*. New York, NY: Oxford University Press.

Towse, J. N., & Hitch, G. J. (1995). Is there a relationship between task demand and storage space in tests of working memory capacity? *The Quarterly Journal of Experimental Psychology, 48A*(1), 108–124.

Uhlhaas, P. J., Roux, F., Rodriguez, E., Rotarska-Jagiela, A., & Singer, W. (2010). Neural synchrony and the development of cortical networks. *Trends in Cognitive Science, 14*(2), 72–80.

Vogel, E. K., Woodman, G. F., & Luck, S. J. (2001). Storage of features, conjunctions, and objects in visual working memory. *Journal of Experimental Psychology: Human Perception and Performance, 27,* 92–114.

Wass, S. V., Scerif, G., & Johnson, M. J. (2012). Training attentional control and working memory - Is younger, better? *Developmental Review, 32*(4), 360–387.

Wei, Z., Wang, X.-J., & Wang, D.-H. (2012). From distributed resources to limited slots in multiple-item working memory: a spiking network model with normalization. *Journal of Neuroscience, 32,* 11228–11240. doi:10.1523/JNEUROSCI. 0735-12.2012

Wheeler, M., & Treisman, A. M. (2002). Binding in short-term visual memory. *Journal of Experimental Psychology: General, 131,* 48–64.

Xu, Y., & Chun, M. M. (2006). Dissociable neural mechanisms supporting visual short-term memory for objects. *Nature, 440,* 91–95.

Zhang, W., & Luck, S. J. (2008). Discrete fixed-resolution representations in visual working memory. *Nature, 453,* 233–235.